Tunable Microwave Filters and Phase Shifters Based on Ferromagnetic/Dielectric Multilayer Waveguides

Jiashu Zhang, Jinzhu Zhao, Ruwen Peng*, Jia Li, Ruili Zhang, and Mu Wang

National Laboratory of Solid State Microstructures and Department of Physics, Nanjing University, Nanjing 210093, China

Received November 10, 2009; accepted January 6, 2010; published online March 23, 2010

We present theoretically microwave filters and phase shifters based on the propagation of hybrid electromagnetic-spin waves in a ferromagnetic/dielectric multilayer waveguide. It is demonstrated that some propagating modes of microwave appear in the waveguide and the number of the modes increases with increasing the number of the building blocks. Those propagating modes originate from the coupling between microwave and spin wave, associated with the collective excitations of spin motions in the whole multilayer system when the layer thickness is relatively thin. In addition, it is shown that the attenuation of microwaves and phase difference in the waveguide are tuned by the magnetic field, the ferromagnetic resonance line width, and the conductivity of ferromagnetic material. The investigations can be used in designing tunable compact bandpass filters and phase shifters of microwave.

DOI: 10.1143/JJAP.49.033004

1. Introduction

There has been increasing interest in high-frequency electromagnetic wave devices in recent years.[1–10] Particularly, microwave bandpass filters and phase shifters achieve significant applications on satellite and mobile communication, security and military. It is known that semiconductors, ferroelectrics and ferrites can be applied in bandpass filters and phase shifters of microwave. For example, microstrip notch filters can be made by using metallic magnetic materials,[6] where the input signal is absorbed strongly at the resonant frequency of the ferromagnet. And based on magnetic microstrip, local band pass filters have been experimentally realized.[7] Very recently, hexagonal ferrites have been theoretically proposed for use in microwave notch filters and phase shifters.[10]

Tunable magnetic devices for signal processing are usually in bulk. Microwave filters based on yttrium iron garnet (YIG) need very large external magnetic field to operate. Instead, because of the high saturation magnetism in thin films, metallic magnetic thin films are now being studied widely.[11,12] By varying magnetic field, strong magnetic response can be adjusted at ferromagnetic resonance (FMR) frequency, which makes them possible to become microwave devices.[13–15]

In this work, we propose ferromagnetic (FM)/dielectric (DE) multilayer waveguides to use as tunable microwave filters and phase shifters. The multilayer film is sandwiched by thick silver films, and it is constructed by repeating a building block, which contains a FM layer and a DE layer. Microwave mainly propagates in the dielectric layers, while the spin wave is excited in the FM layers. In the FM/DE multilayer system, the excitations of spin wave in individual layer are coupled each other by the tail of evanescent field. If the layer thickness is relatively thin, the coupling of the spin wave definitely affects on the microwave propagation. In this work, we show that some propagating modes of microwave indeed appear in the FM/DE multilayer waveguide and the number of the modes increases with increasing the number of the building blocks. Those propagating modes originate from the coupling between microwave and spin wave. Furthermore, the attenuation of microwave and phase difference in the waveguides are tuned by the magnetic field, the FMR line width, and ferromagnetic conductivity. The investigations can be used in designing tunable compact bandpass filters and phase shifters of microwave.

2. Theoretical Model

The propagation of the electromagnetic waves in the waveguide obeys Maxwell equations as

$$\nabla \times (\nabla \times \mathbf{H}) = -\frac{1}{c^2}\frac{\partial^2}{\partial t^2}(\boldsymbol{\varepsilon}\boldsymbol{\mu}\mathbf{H}), \tag{1}$$

where $\mathbf{H}$ is the magnetic field, and usually the permittivity tensor $\boldsymbol{\varepsilon}$ and the permeability tensor $\boldsymbol{\mu}$ take the form of

$$\boldsymbol{\varepsilon} = \begin{bmatrix} \varepsilon_{11} & \varepsilon_{12} & \varepsilon_{13} \\ \varepsilon_{21} & \varepsilon_{22} & \varepsilon_{23} \\ \varepsilon_{31} & \varepsilon_{32} & \varepsilon_{33} \end{bmatrix}, \tag{2}$$

$$\boldsymbol{\mu} = \begin{bmatrix} \mu_{11} & \mu_{12} & \mu_{13} \\ \mu_{21} & \mu_{22} & \mu_{23} \\ \mu_{31} & \mu_{32} & \mu_{33} \end{bmatrix}. \tag{3}$$

By assuming $\mathbf{H}(\mathbf{t}) = \mathbf{H}e^{i(\mathbf{kx}-\omega t)}$ (where $\mathbf{k}$ is the wave vector and ω is angular frequency), we have

$$\begin{bmatrix} k_y^2 + k_z^2 - \frac{\omega^2}{c^2}\sum_{m=1}^{3}\varepsilon_{1m}\mu_{m1} & -k_xk_y - \frac{\omega^2}{c^2}\sum_{m=1}^{3}\varepsilon_{1m}\mu_{m2} & -k_xk_z - \frac{\omega^2}{c^2}\sum_{m=1}^{3}\varepsilon_{1m}\mu_{m3} \\ -k_xk_y - \frac{\omega^2}{c^2}\sum_{m=1}^{3}\varepsilon_{2m}\mu_{m1} & k_x^2 + k_z^2 - \frac{\omega^2}{c^2}\sum_{m=1}^{3}\varepsilon_{2m}\mu_{m2} & -k_yk_z - \frac{\omega^2}{c^2}\sum_{m=1}^{3}\varepsilon_{2m}\mu_{m3} \\ -k_xk_z - \frac{\omega^2}{c^2}\sum_{m=1}^{3}\varepsilon_{3m}\mu_{m1} & -k_yk_z - \frac{\omega^2}{c^2}\sum_{m=1}^{3}\varepsilon_{3m}\mu_{m2} & k_x^2 + k_y^2 - \frac{\omega^2}{c^2}\sum_{m=1}^{3}\varepsilon_{3m}\mu_{m3} \end{bmatrix} \begin{bmatrix} H_x \\ H_y \\ H_z \end{bmatrix} = \begin{bmatrix} 0 \\ 0 \\ 0 \end{bmatrix}. \tag{4}$$

*E-mail address: rwpeng@nju.edu.cn

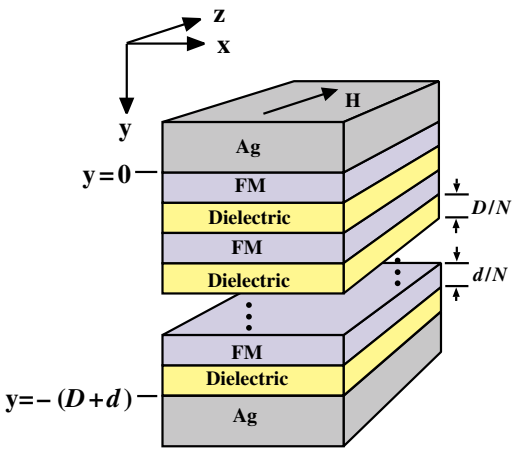

Fig. 1. (Color online) The schematic FM/DE multilayer waveguide. In the waveguide, the multilayer is constructed by repeating a building block, which contains a ferromagnetic layer and a dielectric layer. The whole multilayer is sandwiched by thick silver films. An external magnetic field (H) is applied parallel to the z direction, along which the microwave propagates. The number of building blocks in the multilayer structure is N. The total thickness of the FM layers is set as d, while the total thickness of the dielectric layers is set as D.

The matrix in eq. (4) can be defined as $\mathbf{Q}$, then eq. (4) has a nontrivial solution only if the determinant of $\mathbf{Q}$ is zero, which gives a dispersion relationship in the system.

For the simplification, we consider a planar multilayer waveguide schematically shown in Fig. 1, where thick silver layers are on both top and bottom. The external magnetic field H_{ext} is applied along the z-axis, and the waveguide extends from $x = -\infty$ to $+\infty$, the edge effect can be ignored in the x direction. Thereafter, we have $k_x = 0$ due to the symmetry in the waveguide. Usually for the FM layer or the dielectric layer, the permittivity tensor has the diagonal form as

$$\boldsymbol{\varepsilon} = \begin{bmatrix} \varepsilon_1 & 0 & 0 \\ 0 & \varepsilon_2 & 0 \\ 0 & 0 & \varepsilon_3 \end{bmatrix}. \tag{5}$$

We define a combination of $\boldsymbol{\varepsilon}$ and $\boldsymbol{\mu}$ as

$$\boldsymbol{Z} = \begin{bmatrix} \zeta_{11} & \zeta_{12} & \zeta_{13} \\ \zeta_{21} & \zeta_{22} & \zeta_{23} \\ \zeta_{31} & \zeta_{32} & \zeta_{33} \end{bmatrix} = \boldsymbol{\varepsilon}\boldsymbol{\mu}. \tag{6}$$

Then, the determinant $|\boldsymbol{Q}| = 0$ can be rewritten as

$$\begin{aligned} &-\zeta_{22}{k_y}^4 - (\zeta_{23}+\zeta_{32})k_z{k_y}^3 + \left[\frac{\omega^2}{c^2}(\mathbf{Z}_{11}+\mathbf{Z}_{33}) - (\zeta_{22}+\zeta_{33}){k_z}^2\right]{k_y}^2 \\ &+ \left[\frac{\omega^2}{c^2}(\mathbf{Z}_{23}+\mathbf{Z}_{32})k_z - (\zeta_{23}+\zeta_{32}){k_z}^3\right]k_y - \zeta_{33}{k_z}^4 + \frac{\omega^2}{c^2}(\mathbf{Z}_{11}+\mathbf{Z}_{22}){k_z}^2 - \frac{\omega^4}{c^4}\det\mathbf{Z} = 0. \end{aligned} \tag{7}$$

For a given k_z, there exist four roots of k_y. Therefore, the magnetic filed in the structure is expressed as

$$\begin{cases} H_x = \sum_{j=1}^{4} A(j)e^{ik_y(j)y}e^{ik_z z} \\ H_y = \sum_{j=1}^{4} \alpha(j)A(j)e^{ik_y(j)y}e^{ik_z z} \\ H_z = \sum_{j=1}^{4} \beta(j)A(j)e^{ik_y(j)y}e^{ik_z z} \end{cases}, \tag{8}$$

where the parameters α and β are determined by the matrix $\mathbf{Q}$. Besides, the electric field in the structure can be obtained based on

$$\boldsymbol{\varepsilon}^{-1}\nabla \times \mathbf{H} = \frac{1}{c}\frac{\partial \mathbf{E}}{\partial t}. \tag{9}$$

Therefore, the electromagnetic field in the FM layer or the dielectric layer can be obtained. At the interface between the FM layer and the dielectric one, the tangential components of $\mathbf{E}$ and $\mathbf{H}$ are continuous. In addition, it is assumed that the electromagnetic wave does not enter the thick silver layers in the waveguide. For convenience, we define a coordinate system such that all the interfaces of multilayer structure are parallel to the x–z plane, and the top of the first ferromagnetic layer as $y = 0$ as shown in Fig. 1. The number of building blocks in the multilayer structure is N. The total thickness of the FM layers is set as d, while the total thickness of the dielectric layers is set as D. Thus the bottom of the dielectric layer is chosen to be $y = -(D+d)$. Based on the boundary condition, we have four equations: at $y = 0$, there are $E_x = 0$ and $E_z = 0$; while at $y = -(D+d)$, there are also $E_x = 0$ and $E_z = 0$. Thereafter, it is possible to find numerically the solutions of k_z for a given ω and give the dispersion curves in the waveguide.

3. Numerical Results and Discussion

Based on the above theoretical analysis, we can numerically study the microwave propagation in our FM/DE multilayer waveguides. Note that the total thicknesses of the dielectric layer (D) and the FM layer (d) are kept as constants in all waveguides, respectively. Then, in each waveguide, the thickness of the dielectric layer is D/N and the thickness of the FM layer is d/N, respectively. Here N is the repeating number of the building blocks. In the following calculation, we choose Fe as the FM material and GaAs as the dielectric one. The permeability tensor $\boldsymbol{\mu}$ in Fe is of this form:

$$\boldsymbol{\mu} = \begin{bmatrix} \mu_1 & i\mu_t & 0 \\ -i\mu_t & \mu_1 & 0 \\ 0 & 0 & 1 \end{bmatrix}, \tag{10}$$

with

$$\mu_1 = 1 + \frac{4\pi\gamma M\omega_0}{{\omega_0}^2 - \omega^2} \quad \text{and} \quad \mu_t = \frac{4\pi\gamma M\omega}{{\omega_0}^2 - \omega^2}.$$

Here $\omega_0 = \gamma H - i\Gamma\omega$, where γ is the gyromagnetic ratio and M is the saturation magnetization. The FMR line width ΔH, depends upon the dimensionless parameter Γ as[2,16]

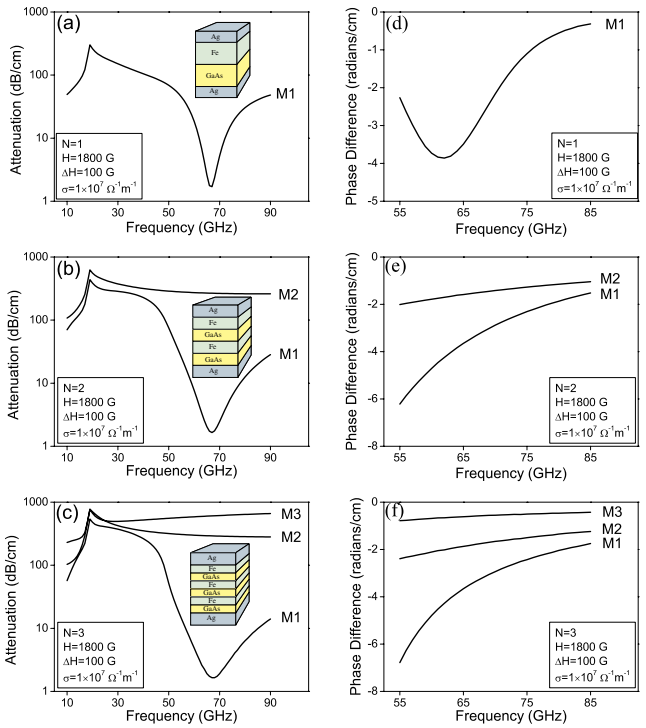

Fig. 2. (Color online) Microwave attenuation and phase difference as a function of frequency in the Fe/GaAs multilayer waveguides with different number of building blocks N. (a,d) $N = 1$; (b,e) $N = 2$; (c,f) $N = 3$. The insert is a schematic waveguide in each case. Here, the total thickness of the dielectric layer is kept as $D = 1\,\mu$m, and the total thickness of the ferromagnetic layer is kept as $d = 1\,\mu$m in each waveguide, respectively.

$$\Delta H = 1.16\left(\frac{\omega}{\gamma}\right)\Gamma, \tag{11}$$

where ΔH is in kG, and γ is 2.87 GHz/kG.

3.1 Microwave attenuation and phase shift in the waveguide

We have calculated the microwave attenuation as a function of frequency in several Fe/GaAs multilayer waveguides as shown in Figs. 2(a)–2(c). In each waveguide, there exists a propagating mode called "M1", which has minimum attenuation near the frequency of 70 GHz. This feature agrees with the previous result in the sandwich.[2)] Physically, both the external magnetic field and the saturation magnetization determine the attenuation frequency and the minimum attenuation value. More interestingly, with increasing the number of building blocks, more propagating modes appear at the GHz frequencies, which originate from the coupling between microwave and spin wave in the FM/DE multilayer structure. For example, there are two propagating modes (M1 and M2) in the waveguide with $N = 2$ as shown in Fig. 2(b); and three propagating modes (M1, M2, and M3) in the waveguide with $N = 3$ as shown in Fig. 2(c). Compared with the mode M1, the other modes do not have minimum attenuation near the frequency of 70 GHz. In general, there are N groups of propagating modes in the FM/DE waveguide when there are N building blocks, thereafter, multiple band pass regions are demonstrated in those waveguides.

The phase difference of microwave signal in the Fe/GaAs multilayer waveguide with different N is also illustrated as a function of frequency as shown in Figs. 2(d)–2(f). Here, phase difference is calculated for an external field of 1800 G, compared to zero external field. According to theoretical analysis, the imaginary part of k_z in eq. (4) changes the attenuation of microwave signal in the waveguide, while the real part of k_z determines the phase difference of microwave. When the number of building blocks is changed in the waveguide, the coupling between microwave and spin wave will be different in the structure, which eventually influences the propagating modes (related to k_z). As shown in Figs. 2(d)–2(f), the curve of the phase difference changes dramatically its shape with increasing the number of building blocks. It is illustrated that the phase differences of microwaves are distinct for different modes, but for each mode, π phase shift can be achieved at several centimeters in the waveguide. This feature makes it possible to use the present FM/DE waveguides to achieve available phase shift of microwave.

In order to demonstrate the coupling between microwave and spin wave in the FM/DE multilayer waveguides, we have calculated the spatial distributions of electromagnetic fields in the structure. Figure 3 illustrates the calculated energy flux S and the distributions of both H_x and E_z in the Fe/GaAs waveguide with $N = 1$, where the microwave frequency is set to be 40 GHz. It is obvious that the electromagnetic energy is mainly confined in the GaAs layer [Fig. 3(a)], which demonstrates that the dielectric layer indeed support the waveguide mode. Besides, the electromagnetic wave penetrates into the Fe layer as shown in Figs. 3(b) and 3(c). Then the spin motions in the FM layer are excited by the tail of evanescent field, which implies that the FM layer supports collective excitations (spin waves). Along the propagating direction (z axis), both H_x [Fig. 3(b)] and E_z [Fig. 3(c)] become weakened. And along y axis, H_x attenuates more rapidly in the Fe layer than that in the GaAs layer. As for E_z, it attenuates in both Fe and GaAs layers.

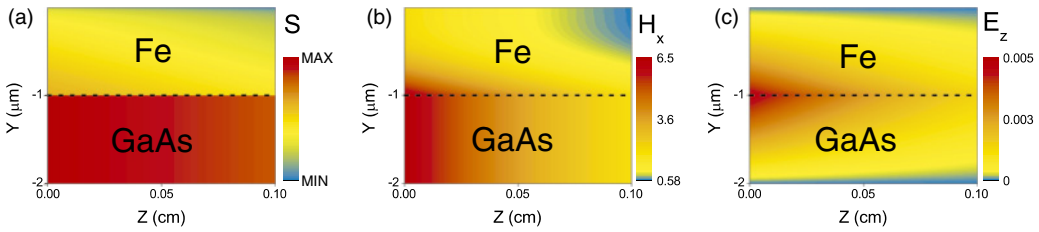

Fig. 3. (Color online) The spacial distributions of the electromagnetic flux S (a), the magnetic field H_x (b), and the electric field E_z (c) in the Fe/GaAs multilayer waveguide with $N = 1$, where the microwave frequency is set to be 40 GHz. The dotted line represents the interface between ferromagnetic and dielectric layers. The parameters in the calculation are set as follows: $H = 1800$ G, $\sigma = 1 \times 10^7\ \Omega^{-1}\ \mathrm{m}^{-1}$, $\Delta H = 100$ G. The propagation distance for microwave is chosen to be 0.1 cm.

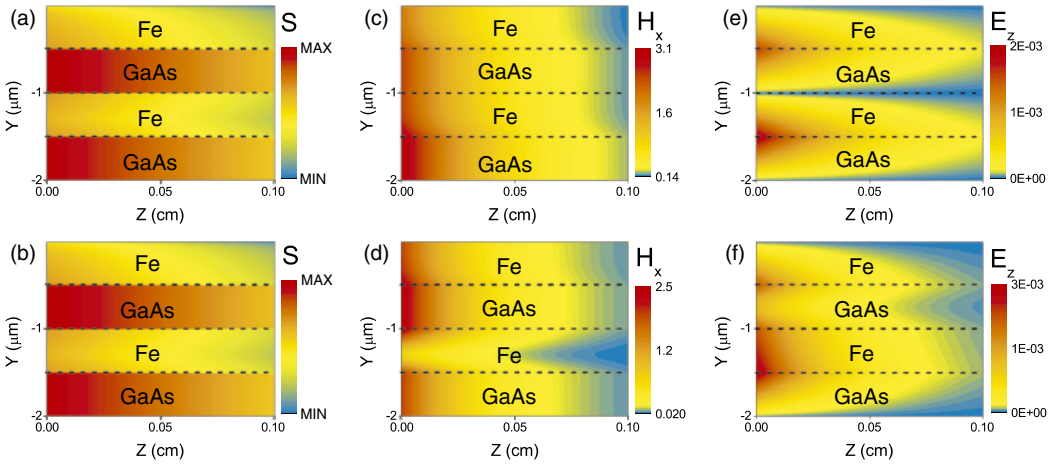

Fig. 4. (Color online) The spacial distributions of the electromagnetic flux S, the magnetic field H_x, and the electric field E_z for two types of propagating modes [M1 and M2 marked in Fig. 2(b)] in the Fe/GaAs multilayer waveguide with $N = 2$. For mode M1: (a) S, (c) H_x, and (e) E_z; while for mode M2: (b) S, (d) H_x, and (f) E_z. The microwave frequency is set to be 40 GHz, other parameters are the same as Fig. 3.

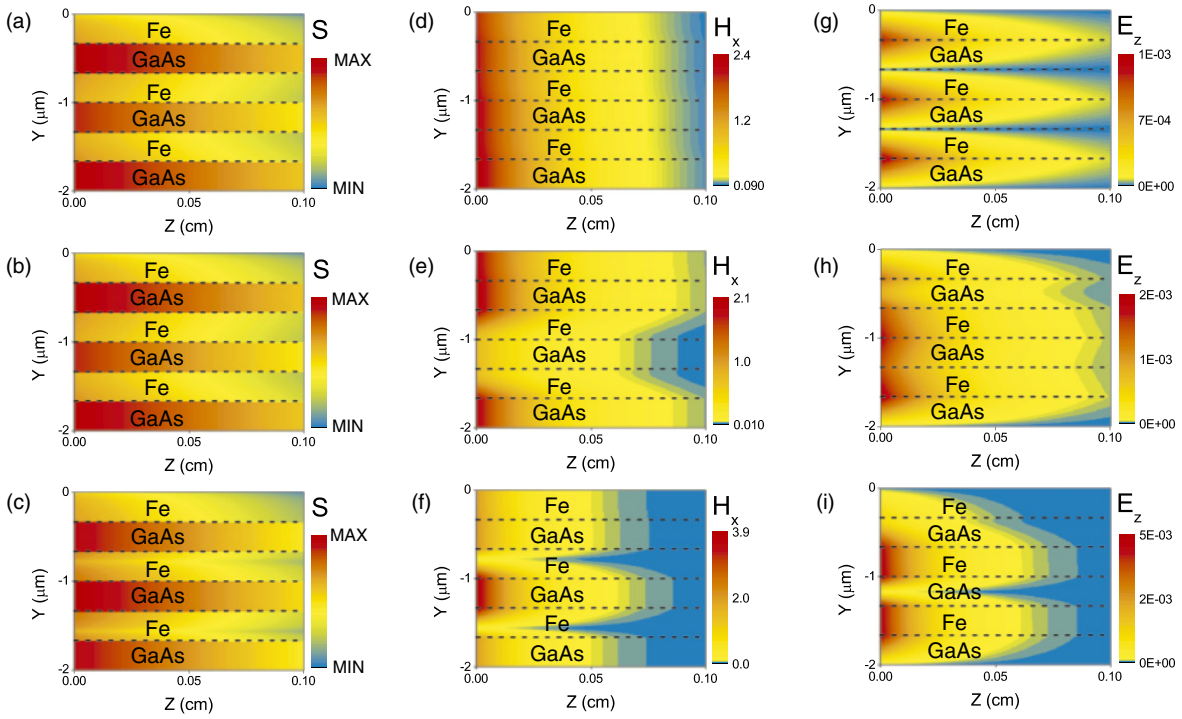

Fig. 5. (Color online) The spacial distributions of the electromagnetic flux S, the magnetic field H_x, and the electric field E_z for three types of propagating modes [M1, M2, and M3 marked in Fig. 2(c)] in the Fe/GaAs multilayer waveguides with $N = 3$. For mode M1: (a) S, (d) H_x, and (g) E_z; for mode M2: (b) S, (e) H_x, and (h) E_z; for mode M3: (c) S, (f) H_x, and (i) E_z. The microwave frequency is set to be 40 GHz; other parameters are the same as Fig. 3.

All these components contribute to the energy flux in the waveguide.

Actually, the coupling between microwave and spin wave is strongly dependent of the FM/DE multilayer structure. Figures 4 and 5 illustrate the calculated energy flux S and the distributions of H_x and E_z in the waveguides with $N = 2$ and 3, respectively. In the Fe/GaAs multilayer waveguide with $N = 2$, there are two types propagating modes, i.e., M1 and M2. For both M1 and M2, the energy flux mainly concentrates in the dielectric layers [Figs. 4(a) and 4(b)]. The field distributions in Figs. 4(c)–4(f) demonstrate that the collective excitations of spin wave are coupled with the microwave and affected the microwave propagation. While three types propagating modes exist in the Fe/GaAs multilayer waveguide with $N = 3$, i.e., M1, M2, and M3. For each mode, the energy flux indeed mainly concentrates in the dielectric layers [Figs. 5(a)–5(c)]. However, for different modes, the excitation of spin wave and its coupling with the microwave are quite different based on the electric and magnetic spacial distributions shown in Figs. 5(d)–5(i). This feature further demonstrates that spin wave indeed works as collective excitation and couples with the microwave in the FM/DE multilayer waveguide.

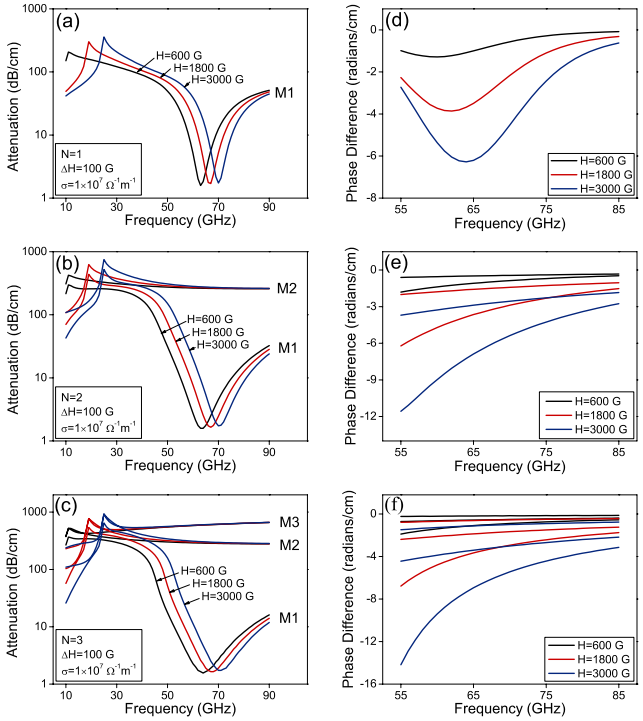

Fig. 6. (Color online) Microwave attenuation and phase shift as a function of frequency in the Fe/GaAs multilayer waveguides at different external magnetic fields (H). The waveguide has the number of building blocks: (a,d) $N = 1$; (b,e) $N = 2$; (c,f) $N = 3$, respectively.

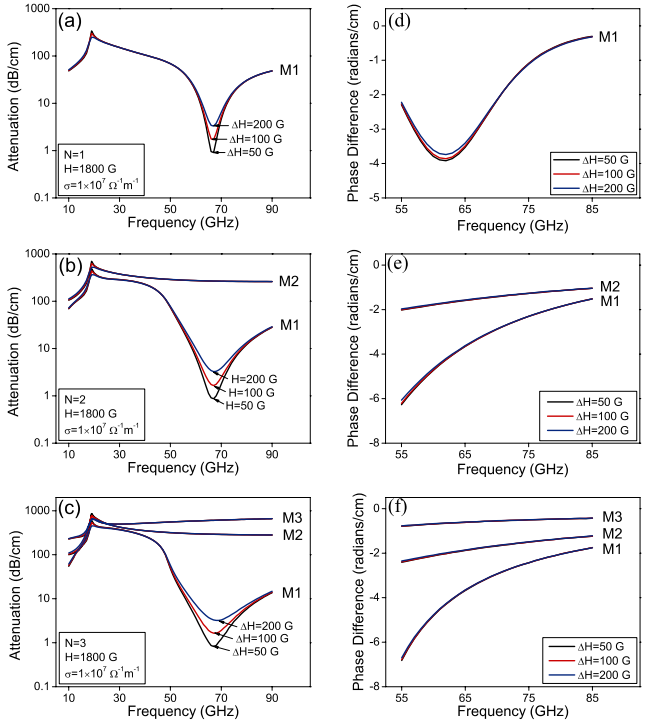

Fig. 7. (Color online) Microwave attenuation and phase shift as a function of frequency in the Fe/GaAs multilayer waveguides at different FMR line widths (ΔH). The waveguide has the number of building blocks: (a,d) $N = 1$; (b,e) $N = 2$; (c,f) $N = 3$, respectively.

3.2 Tuning microwave attenuation and phase shift in the waveguide

It is valuable to tune the microwave filters and phase shifts in the FM/DE multilayer waveguide. Based on the theoretical analysis, it is possible to study how the attenuation of microwaves and phase difference in the waveguide affect on the external magnetic field, the FMR line width, and ferromagnetic conductivity, respectively.

Figure 6 illustrates the microwave attenuation and phase difference as a function of frequency in the Fe/GaAs waveguides when the external magnetic field is changed. With increasing the external magnetic field, the FMR frequency of the FM layers is moved to higher frequency, thereafter, the band pass region is also is shifted to higher frequency as shown in Figs. 6(a)–6(c). However, the external magnetic field has little effect on the amplitude of attenuation. When the number of building blocks increases, the magnetic field shifts the propagation mode, without altering the shape of the attenuation curve, which makes it possible to use those multilayer waveguides to achieve tunable band pass filter. Meanwhile, increasing external field can significantly enlarge the phase difference of microwave in the waveguide [Figs. 6(d)–6(f)]. Besides, the phase gap between different modes can also be enlarged by the applied magnetic field [for example, Figs. 6(e) and 6(f)]. Therefore, by changing the external magnetic field, we can tune the band pass of microwave and also the phase shift in the FM/DE multilayer waveguides.

The microwave attenuation as a function of frequency for different FMR line width is demonstrated in the Fe/GaAs multilayer waveguides as shown in Figs. 7(a)–7(c). The FMR line width has little effect on broadening the band pass region; however, the amplitude of the minimum attenuation has been changed apparently. Far away from the band pass region, the effect on microwave attenuation can be neglected. Anyway, our calculation demonstrates that the phase shift can not be effectively altered by the FMR line width [Figs. 7(d)–7(f)].

Besides, it is interesting to show how the ferromagnetic conductivity influences the microwave attenuation and the phase shift in the Fe/GaAs multilayer waveguide. As shown in Figs. 8(a)–8(c), with increasing the ferromagnetic conductivity, the maximum attenuation of microwave is decreased and the width of the minimum attenuation is reduced. Meanwhile, the lower conductivity can improve the phase difference as shown in Figs. 8(d)–8(f). When the conductivity is decreased, the phase shift becomes larger in the waveguides, and the phase difference of microwave among different modes is enlarged. Obviously, this feature may have potential applications in designing tunable phase shifters.

4. Conclusions

We have theoretically studied microwave filters and phase shifters based on the propagation of hybrid electromagnetic-spin waves in a FM/DE multilayer waveguide. It is demonstrated that some propagating modes of microwave appear in the waveguide and the number of the modes increases with increasing the number of the building block. Those propagating modes originate from the coupling between microwave and spin wave, associated with the collective excitations of spin motions in the whole multilayer system when the layer thickness is relatively thin. In addition, it is shown that the attenuation of microwaves and

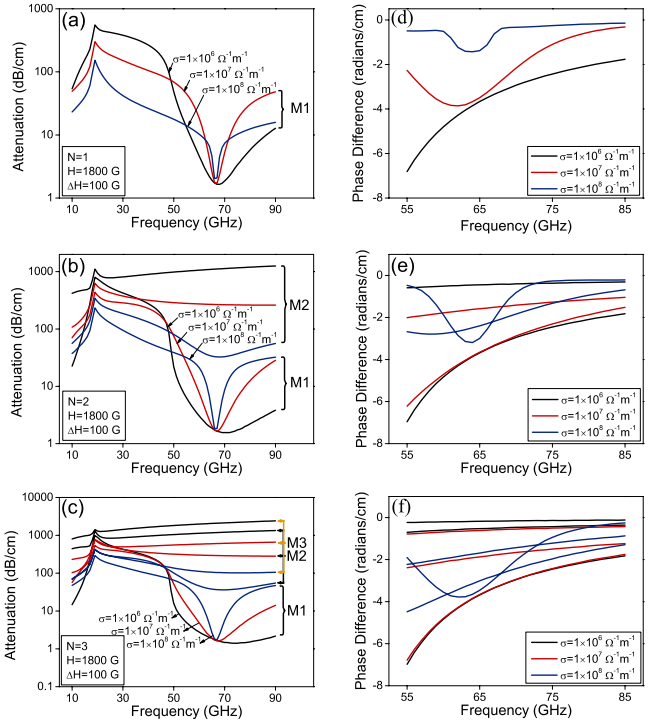

Fig. 8. (Color online) Microwave attenuation and phase shift as a function of frequency in the Fe/GaAs multilayer waveguides at different ferromagnetic conductivities (σ). The waveguide has the number of building blocks: (a,d) $N = 1$; (b,e) $N = 2$; (c,f) $N = 3$, respectively.

phase difference in the waveguide are tuned by the magnetic field, the FMR line width, and ferromagnetic conductivity. The investigations can be used in designing tunable compact bandpass filters and phase shifters of microwave.

Acknowledgments

This work was supported by grants from the NSF of China (Grant Nos. 10625417, 10874068, and 10904061), the MOST of China (Grant Nos. 2004CB619005 and 2006CB921804), and partly by Jiangsu Province (Grant No. BK2008012).

1) R. E. Camley and D. L. Mills: J. Appl. Phys. **82** (1997) 3058.
2) R. J. Astalos and R. E. Camley: J. Appl. Phys. **83** (1998) 3744.
3) N. Cramer, D. Lucic, R. E. Camley, and Z. Celinski: J. Appl. Phys. **87** (2000) 6911.
4) S. S. Kang: Phys. Rev. B **65** (2002) 064401.
5) B. Kuanr, L. Malkinski, R. E. Camley, Z. Celinski, and P. Kabos: J. Appl. Phys. **93** (2003) 8591.
6) B. Kuanr, Z. Celinski, and R. E. Camley: Appl. Phys. Lett. **83** (2003) 3969.
7) B. Kuanr, D. L. Marvin, T. M. Christensen, R. E. Camley, and Z. Celinski: Appl. Phys. Lett. **87** (2005) 222506.
8) X. F. Zhang, R. W. Peng, S. Kang, L. S. Cao, R. L. Zhang, Mu Wang, and A. Hu: J. Appl. Phys. **100** (2006) 063911.
9) A. B. Ustinov, G. Srinivasan, and B. A. Kalinikos: Appl. Phys. Lett. **90** (2007) 031913.
10) T. J. Fal and R. E. Camley: J. Appl. Phys. **104** (2008) 023910.
11) E. Schloemann, R. Tutison, J. Weissman, H. J. Van Hook, and T. Vatimos: J. Appl. Phys. **63** (1988) 3140.
12) V. S. Liau, T. Wong, W. Stacey, S. Ali, and E. Schloemann: IEEE MTT-S Int. Microwave Symp. Dig., 1991, Vol. 3, p. 957.
13) I. Huynen, G. Goglio, D. Vanhoenacker, and A. Vander Vorst: IEEE Microwave Guided Wave Lett. **9** (1999) 401.
14) C. S. Tsai, J. Su, and C. C. Lee: IEEE Trans. Magn. **35** (1999) 3178.
15) N. Cramer, D. Lucic, D. K. Walker, R. E. Camley, and Z. Celinski: IEEE Trans. Magn. **37** (2001) 2392.
16) B. Heinrich and J. F. Cochran: Adv. Phys. **42** (1993) 523.